JOURNAL OF MATERIALS SCIENCE **31** (1996) 5113–5118

Pyrolytic behaviour of Si–Ti–C–O fibre in alumina powder

T. SHIMOO, K. OKAMURA
Department of Metallurgy and Materials Science, College of Engineering, Osaka Prefecture University, 1-1 Gakuen-cho, Sakai-shi, Osaka-fu 593, Japan

In relation to the synthesis of a ceramic matrix composite reinforced by Si–Ti–C–O fibre (Tyranno), the pyrolysis of Tyranno in alumina powder was investigated at temperatures, *T*, of 1773–1973 K under Ar or N_2 atmosphere. Using a Tyranno–alumina compact, pyrolytic rates were determined with a thermobalance. The heat-treated fibres were examined by X-ray diffraction (XRD) and scanning electron microscope (SEM) observation. Under N_2 atmosphere and at lower temperatures, pyrolysis of Tyranno was retarded by the formation of a nitrided case. The retardness effect disappeared in the presence of alumina powder. At elevated temperatures, pyrolysis was suppressed by the presence of alumina powder. Alumina was reduced to be nitrided into AlN by the gas-phase reaction between the pyrolytic gas, CO and N_2. In addition,Tyranno crystallized into β-SiC and α-SiC of type 2H.

1. Introduction

Polymer-derived SiC fibres are of interest as reinforcing fibres with metal- and ceramic–matrix composites [1, 2]. The fibres contain substantial amounts of oxygen, as well as carbon, beyond the stoichiometric ratio of SiC, and are in an amorphous state. As the fibres are thermodynamically unstable at elevated temperatures, they have a tendency to crystallize into β-SiC, generating SiO and CO [3–6]. Such pyrolysis, results in remarkable reduction of fibre strength. In the synthesis of ceramic composites, the fibre–ceramic powder mixture is heated to high temperature. Before sintering densely, the reinforcing fibres deteriorate; probably due to pyrolysis. The pyrolytic behaviour of the fibres in ceramic powder is considered to differ from that of the fibre alone. Previously, an investigation has not been undertaken on this subject. The authors have investigated the pyrolytic behaviour of Si–C–O fibre (Nicalon) in alumina powder [7, 8] and Si–C–O fibre (Nicalon) in Si_3N_4 powder [9].

In the present work, pyrolysis of the Si–Ti–C–O fibre in alumina powder was studied under both Ar and N_2 atmosphere. Furthermore, the investigations were performed with the nitridation of the fibre, the evaporation of alumina and the formation of AlN, which proceeded as side reactions simultaneously to pyrolysis of the fibre.

2. Experimental procedure

The SiC fibre used is composed of Si–Ti–C–O fibres (trade name: Tyranno) produced by Ube Industries Co. It has a composition of $SiTi_{0.02}C_{1.33}O_{0.44}$ and mean diameter of 8.5 μm. The fibre was heated at 1073 K for 3.6 ks under Ar atmosphere, in order to remove the sizing agent. The alumina powder used has a purity higher than 99% and a mean diameter of 2.1 μm. Some 0.5 g of Tyranno and 0.5 g of alumina were mixed thoroughly in an alumina mortar. The mixture was formed into a tablet of 15 mm diameter by compacting at a pressure of 0.49 MPa.

The thermogravimetry thermobalance unit consists of an analogue-type autorecording balance and a carbon resistance furnace. When the desired temperature was reached, Ar or N_2 was allowed to flow from the bottom of the furnace at a gas flow rate of $2.5 \times 10^{-5}\ m^3\,s^{-1}$. The tablet was charged in a graphite crucible of 16 mm inner diameter and 100 mm depth. The crucible was suspended in the hot zone of the furnace after connecting a graphite rod and a Kantal wire to the balance. The mass loss was continuously recorded during each run. Using the same procedure, thermogravimetric analysis (TGA) of Tyranno alone was conducted as a comparative experiment. After 3.6 ks, the sample was quenched by raising the crucible to the low-temperature zone of the furnace. The reaction products were examined by XRD and by SEM observation.

3. Results

3.1. TGA curves

Fig. 1 shows the TGA curves for Tyranno alone and for the Tyranno–alumina compact heated at 1773 to 1973 K under Ar atmosphere. W_0 and ΔW are the initial mass of fibre and the mass loss determined with a thermobalance, respectively. The mass loss is derived essentially from the pyrolysis of Tyranno. The pyrolysis of Tyranno is retarded by the presence of alumina powder. The effect of retarding the pyrolysis

0022–2461

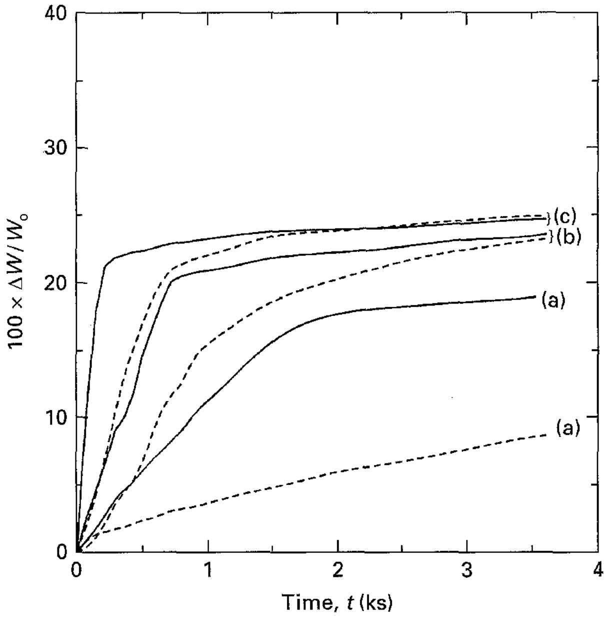

Figure 1 TGA curves for (——) Tyranno alone and (– – –) Tyranno–alumina compact heated under Ar atmosphere at 1773 K (a), 1873 K (b), and 1973 K (c).

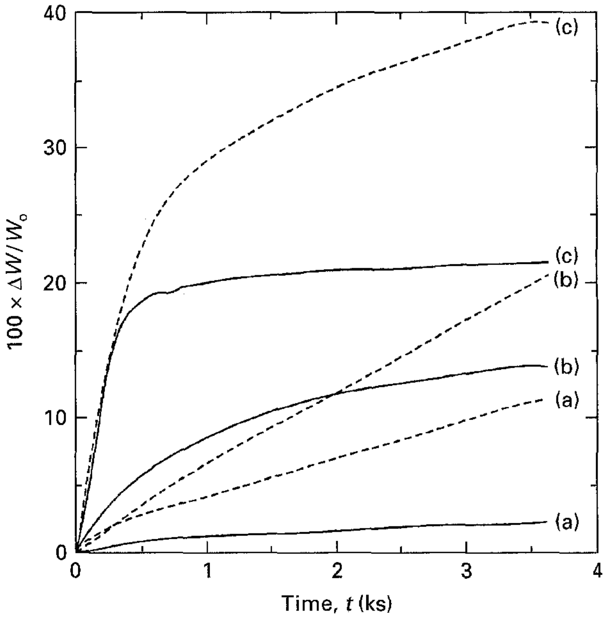

Figure 2 TGA curves for (——) Tyranno alone and (– – –) Tyranno–alumina compact heated under N_2 atmosphere at 1773 K (a), 1873 K (b), and 1973 K (c).

is more significant with a decrease in heating temperature. At 1973 K and in about 2 ks, however, the mass loss becomes larger for the Tyranno–alumina compact than for Tyranno alone. This is because alumina evaporates as Al_2O, as discussed later.

Fig. 2 shows the TGA-curves for Tyranno alone and for the Tyranno–alumina compact heated at 1773–1973 K under N_2 atmosphere. When Tyranno alone is heated, the rapid mass loss occurs at an early stage, and subsequently the gradual mass loss continues. It can be seen from comparison with Fig.1 that the pyrolysis of Tyranno is suppressed under N_2 atmosphere. On the other hand, the Tyranno–alumina compact gives a serious mass loss under N_2 atmosphere. In particular, after heating for 3.6 ks at 1973 K, the value of 100 × $\Delta W/W_0$ is nearly equal to 40 and is roughly double that under Ar atmosphere. Furthermore, it is noteworthy that the mass loss is significantly larger in N_2 than in Ar during heating at 1773 K. These results are attributed to the evaporation of Al_2O and the nitridation of Tyranno, as discussed later.

3.2. X-ray diffraction

Fig. 3 shows XRD patterns of Tyranno and Tyranno–alumina compact heated under Ar atmosphere. The diffraction of the original fibre is broad and is almost in an amorphous state. The diffraction pattern peaks of β-SiC become sharper with rising temperature. The fibre crystallizes highly into β-SiC in the absence of alumina powder. In the Tyranno–alumina compact, crystallization into β-SiC is retarded; though α-SiC, as well as β-SiC, is identified.

Fig. 4 shows XRD patterns of Tyranno and the Tyranno–alumina compact heated under N_2 atmosphere. By comparing Figs 3 and 4, it is found that the crystallization of Tyranno is relatively slower under N_2 than under Ar atmosphere in the absence of alumina powder. In alumina powder, Tyranno crystallizes into a α-SiC and β-SiC. Furthermore, it may be noted that AlN is detected in the Tyranno–alumina compact under N_2 atmosphere.

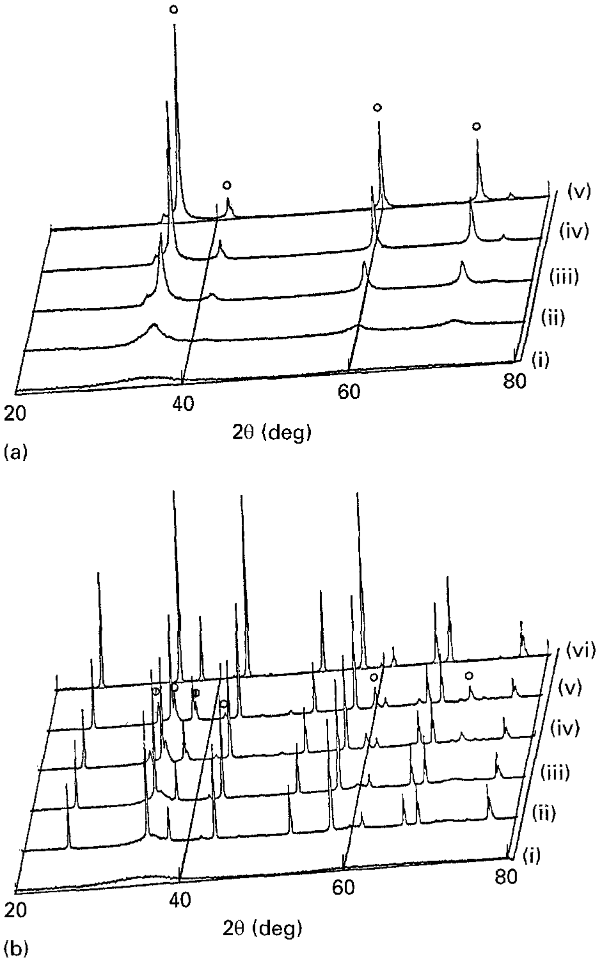

Figure 3 X-ray diffraction patterns of Tyranno alone (a) and Tyranno–alumina compact (b) heated for 3.6 ks under Ar atmosphere. (i) Original fibre, (ii) 1673 K, (iii) 1773 K, (iv) 1873 K, (v) 1973 K, (vi) alumina: (○) β-SiC, (◐) α-SiC.

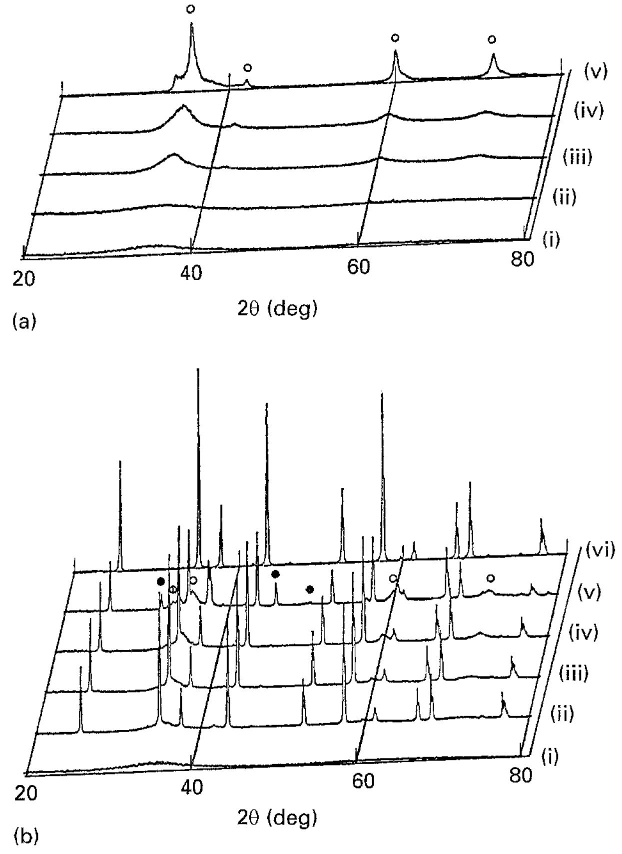

Figure 4 X-ray diffraction patterns of Tyranno alone (a) and Tyranno–alumina compact (b) heated for 3.6 ks under N_2 atmosphere. (i) Original fibre, (ii) 1673 K, (iii) 1773 K, (iv) 1873 K, (v) 1973 K, (vi) alumina: (○) β-SiC, (◐) α-SiC, (●) AlN.

3.3. Appearance of fibre

Fig. 5 shows SEM photographs of Tyranno heated at 1973 K. While SiC crystals are in a microcrystalline state under N_2 atmosphere (Fig. 5b), they coarsen significantly under Ar atmosphere (Fig. 5a). In alumina powder, the fibre has a smooth appearance under both Ar and N_2 atmospheres (Fig. 5c, d). It is evident that the pyrolysis of Tyranno is suppressed under N_2 atmosphere and in alumina powder. Fibre-like deposits are observed on the surface of the Tyranno–alumina compact heated under N_2 atmosphere (Fig. 5). Under Ar atmosphere, however, the deposit is never found on the compact (Fig. 5). These deposits are assumed to be AlN, as discussed later.

4. Discussion

4.1. Pyrolytic behaviour of Tyranno

When Tyranno, which contains 13.6 mass % O and is in an amorphous state, is subjected to elevated temperatures, it tends to crystallize into β-SiC and TiC, involving the generation of both SiO and CO. The pyrolytic reaction is represented by Equation 1.

$$\mathrm{SiTi_{0.02}C_{1.33}O_{0.44}(s)} = 0.935\,\mathrm{SiC(s)} + 0.02\,\mathrm{TiC(s)} + 0.065\mathrm{SiO(g)} + 0.375\,\mathrm{CO(g)} \quad (1)$$

Under Ar atmosphere, the pyrolytic rate is well represented by an Avrami–Erofeev equation and is controlled by the growth of β-SiC crystallites [3–6]. In the presence of alumina powder, pyrolysis of Tyranno is considered to proceed through the following steps

1. nucleation of β-SiC crystallites in Tyranno,
2. growth of β-SiC crystallites accompanying generation of SiO and CO,
3. transfer of SiO and CO from the core to the surface of Tyranno,
4. diffusion of SiO and CO through interparticle pores in the compact, and
5. transfer of SiO and CO from the surface of the compact to the gas phase.

Owing to the sluggishness of step 4, pyrolysis was retarded by the presence of alumina powder (Fig. 1), in the same manner as Nicalon [7].

Under N_2 atmosphere, the pyrolytic behaviour was complicated due to the progress of side reactions; nitridation of Tyranno, evaporation of alumina and formation of AlN. TGA measurement, XRD analysis and SEM observation all indicate that pyrolysis for Tyranno alone proceeds more slowly under N_2 than under Ar atmosphere. A similar result was observed also in the pyrolysis of Si–C–O fibres [7, 8] and the reason seemed to be because the nitrided case formed on the fibre surface under N_2 atmosphere. Upon forming the nitrided case, step 3 can be eventually divided into the following two steps

(i) diffusion of SiO and CO from the core to the nitrided case, and
(ii) diffusion of SiO and CO through the nitrided case.

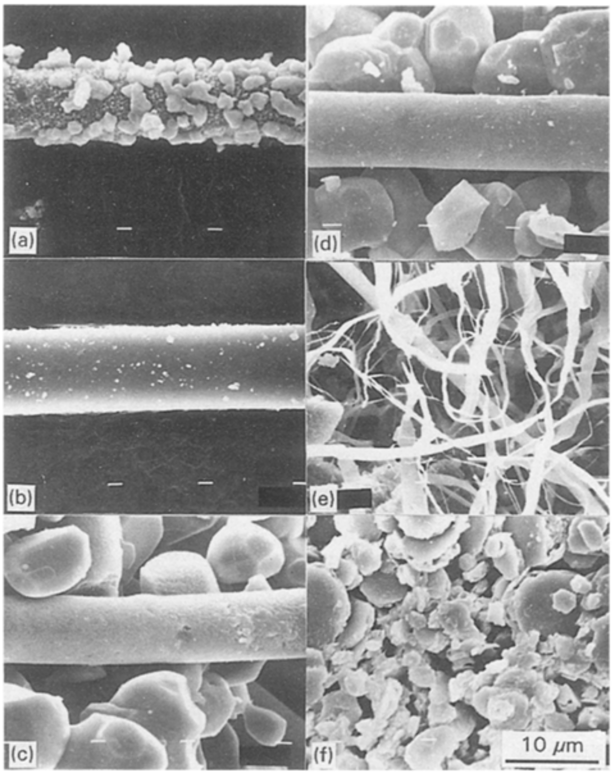

Figure 5 SEM photographs of Tyranno alone (a, b), Tyranno in alumina (c, d), surface of Tyranno–alumina compact (e) and alumina powder alone (f) heated for 3.6 ks at 1973 K under Ar (a, c) and N_2 (b, d–f) atmosphere.

Large resistance of step 3(ii) results in suppressing the pyrolysis of Tyranno. Particularly at lower temperatures, the nitrided case is effective in suppressing the pyrolysis of the core, as shown in Figs 1 and 2. In the presence of alumina powder, however, this effect diminishes, since alumina powder disturbs the access of N_2 to Tyranno, resulting in depression of its nitridation. At 1773 K, therefore, the pyrolysis proceeds faster for the Tyranno–alumina compact than for Tyranno alone (Fig. 2). At elevated temperatures, low partial pressure of N_2 can be achieved on the fibre surface by vigorous generation of SiO and CO and may lead to difficulty in nitriding the fibre. Therefore, at 1973 K, pyrolysis for Tyranno alone is scarcely dependent on the atmosphere. In this way, resistance of step 3(ii) becomes relatively less, and the resistance of step 4 appears sharply. Therefore, XRD patterns show that the pyrolysis of Tyranno is retarded by the presence of alumina powder at 1973 K (Fig. 4), although a vigorous mass loss is observed under N_2 atmosphere (Fig. 2). Thus, under N_2 atmosphere, pyrolysis is retarded by the formation of the nitrided case at lower temperatures; whereas it is retarded by the presence of alumina powder at higher temperatures. A similar result was obtained in a Nicalon/Si_3N_4 compact [9].

After heating at 1973 K for 3.6 ks, the mass loss is larger for Tyranno–alumina than for Tyranno alone (Figs 1 and 2). In particular, this tendency is pronounced under N_2 atmosphere. The mass loss ($100 \times \Delta W/W_0 = 39.5$) exceeds significantly the stoichiometric value ($100 \times \Delta W/W_0 = 23.3$) calculated from the pyrolytic reaction, Equation 1. This indicates that evaporation of alumina and the formation of AlN occur simultaneously with the pyrolysis of Tyranno, and consequently the mass loss is enhanced.

4.2. Evaporation of alumina

Alumina may be reduced by the pyrolytic gases of Tyranno, SiO and CO, to produce a suboxide of aluminium, Al_2O_2 and Al_2O. Thus, first, the reductions of alumina through SiO and their standard free energy change, ΔG^0, are represented by Equations 2 and 3.

$$Al_2O_3(s) + SiO(g) = Al_2O_2(g) + SiO_2(s) \qquad (2)$$

$$\Delta G^0/\mathrm{J\,mol^{-1}} = 414\,890 - 39.92\ T/\mathrm{K} \qquad [10]$$

$$Al_2O_3(s) + 2SiO(g) = Al_2O(g) + 2SiO_2(g) \qquad (3)$$

$$\Delta G^0/\mathrm{J\,mol^{-1}} = -86\,780 + 139.87\ T/\mathrm{K} \qquad [10]$$

For instance, at 1973 K and SiO pressure of 1.01 $\times 10^4$ Pa, the equilibrium pressures of Al_2O_2 and Al_2O are calculated to be 1.27×10^{-5} and 9.88×10^{-3} Pa, respectively. Such low equilibrium pressure indicates Equations 2 and 3 cannot proceed virtually. Therefore, alumina is reduced by CO according to the following reactions

$$Al_2O_3(s) + CO(g) = Al_2O_2(g) + CO_2(g) \qquad (4)$$

$$\Delta G^0/\mathrm{J\,mol^{-1}} = 935\,580 - 212.71\ T/\mathrm{K} \qquad [10]$$

$$Al_2O_3(s) + 2CO(g) = Al_2O(g) + 2CO_2(g) \qquad (5)$$

$$\Delta G^0/\mathrm{J\,mol^{-1}} = 954\,620 - 205.73\ T/\mathrm{K} \qquad [10]$$

From the equilibrium relation for Equations 4 and 5, the partial pressures of Al_2O_2 and Al_2O are dependent on the ratio of p_{CO_2}/p_{CO}

$$p_{Al_2O_2} = K_4/(p_{CO_2}/p_{CO}) \qquad (6)$$

$$p_{Al_2O} = K_5/(p_{CO_2}/p_{CO})^2 \qquad (7)$$

where K_4 and K_5 are equilibrium constants of Equations 4 and 5, respectively. CO_2 reacts with the graphite crucible and free carbon in the fibre to be reproduced in CO

$$C(s) + CO_2(g) = 2CO(g) \qquad (8)$$

$$\Delta G^0/\mathrm{J\,mol^{-1}} = 166\,570 - 171.00\ T/\mathrm{K} \qquad [10]$$

Finally, the p_{CO_2}/p_{CO} ratio of atmosphere is considered to be defined by the equilibrium of Boudouard's reaction, Equation 8. Substituting the value of the equilibrium p_{CO_2}/p_{CO} ratio in Equations 6 and 7, the values of $p_{Al_2O_2}$ and p_{Al_2O} are obtained. Fig. 6 shows the relationship between $p_{Al_2O_2}$, p_{Al_2O} and temperature. At 1773–1973 K, the value of p_{Al_2O} is four to five orders of magnitude higher than $p_{Al_2O_2}$. Therefore, alumina evaporates practically as Al_2O. Figs 4 and 5 indicate that the evaporation of alumina is more vigorous under N_2 than under Ar atmosphere. This is because of the formation of AlN enhances the evaporation of Al_2O as discussed below.

AlN is assumed to be formed on the surface of the Tyranno–alumina compact by the gas-phase reaction (Fig. 3). Thus, Al_2O, which evaporates in alumina powder, diffuses to the surface through interparticle pores, and reacts with N_2 to produce AlN

$$Al_2O(g) + N_2(g) + CO(g) = 2AlN(s) + CO_2(g) \qquad (9)$$

If the evaporation of Al_2O is controlled by diffusion through the interparticle pores, then the evaporation rate, n_{Al_2O}, is given by Equation 10

$$n_{Al_2O} = k_g(p_{Al_2O} - p^*_{Al_2O})/RT \qquad (10)$$

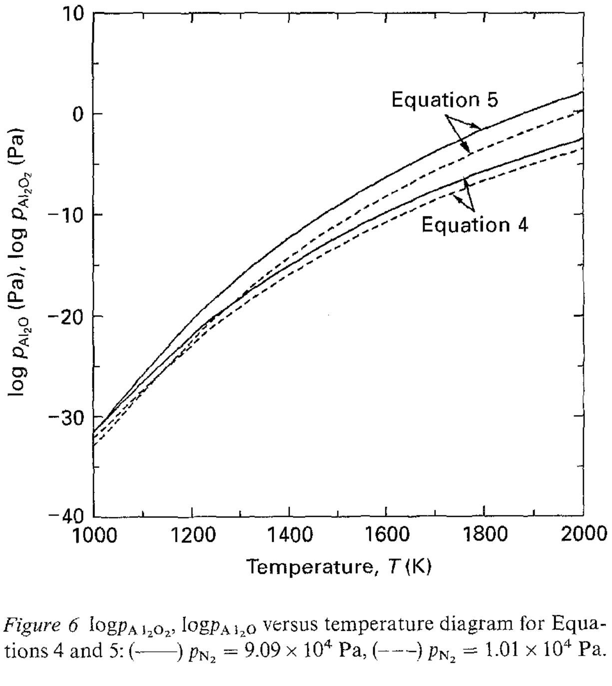

Figure 6 $\log p_{Al_2O_2}$, $\log p_{Al_2O}$ versus temperature diagram for Equations 4 and 5: (——) $p_{N_2} = 9.09 \times 10^4$ Pa, (– – –) $p_{N_2} = 1.01 \times 10^4$ Pa.

where k_g and R are the mass transfer coefficient and gas constant, and p_{Al_2O} and $p^*_{Al_2O}$ are the pressure of Al_2O in the Tyranno–alumina compact and that at the surface of the compact. Under N_2 atmosphere, $p^*_{Al_2O}$ is very small, as Al_2O is consumed by Equation 9. Thus, the value of p_{Al_2O}–$p^*_{Al_2O}$ as the driving force for interparticle diffusion may be considered to be increased, and consequently the evaporation of Al_2O seems to be enhanced.

4.3. Formation of AlN

On the surface of the Tyranno–alumina compact, fibre-like deposits were not observed under Ar atmosphere, but were observed under N_2 atmosphere (Fig. 5). In addition, XRD verified the formation of AlN under N_2 atmosphere (Fig. 4). Therefore, the deposits observed on the compact may be regarded as AlN, which is assumed to be produced by the gas-phase reaction, as mentioned previously. Combining Equations 5 and 9 gives the overall reaction of the AlN formation

$$Al_2O_3(s) + N_2(g) + 3CO(g) = 2AlN(s) + 3CO_2(g) \quad (11)$$

$$\Delta G^0/\mathrm{J\,mol^{-1}} = 190\,250 + 159.91\ T/\mathrm{K} \quad [10]$$

CO_2 is reproduced into CO by Boudouard's reaction, Equation 8. The equilibrium p_{CO_2}/p_{CO} ratios of Equations 8 and 11 were calculated for partial pressures of $p_{N_2} = 9.09 \times 10^4$ and 1.01×10^4 Pa. Fig. 7 represents the relationship between $\log p_{CO_2}/p_{CO}$ for Equations 8 and 11 and temperature. For the experimental temperature range of 1773–1973 K, AlN is produced at a partial pressure of $p_{N_2} = 9.09 \times 10^4$ Pa; while AlN is not produced at a partial pressure of $p_{N_2} = 1.01 \times 10^4$ Pa. Thus, thermodynamical consideration suggests that high partial pressure of N_2 is necessary for the formation of AlN. In the Tyranno–alumina compact, very low partial pressure of N_2, as a consequence of the generation of SiO and CO, prevents the formation of AlN. On the other hand, high partial pressure of N_2 is favourable for the formation of AlN on the surface of the compact.

4.4 Crystallization to α-SiC

When Tyranno alone was heated, it crystallized essentially into β-SiC. On the other hand, on heating in alumina powder, Tyranno crystallized into α-SiC as well as β-SiC under both Ar and N_2 atmosphere. In particular, the XRD pattern of α-SiC was sharp under Ar atmosphere. Identification of the XRD pattern suggests the formation of α-SiC of either type 4H or 15R. While type 4H is stable at temperatures from 1873 to 2373 K, type 15R is unstable over the entire temperature range [11]. In addition, reaction between Al_2O and SiC forms the solid solution of SiC with Al, and consequently α-SiC of type 4H is stabilized [12]. From these considerations, therefore, α-SiC produced by the pyrolysis of Tyranno is confirmed to be of type 4H.

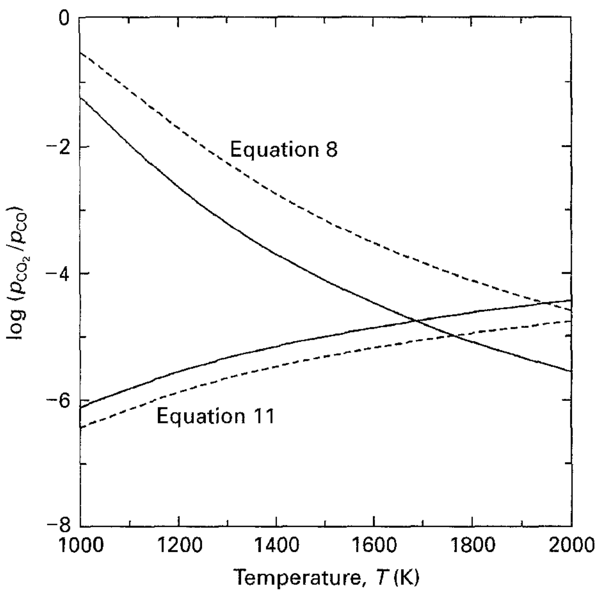

Figure 7 log(p_{CO_2}/p_{CO}) versus temperature diagram for Equations 8 and 11: (——) $p_{N_2} = 9.09 \times 10^4$ Pa, (– – –)$p_{N_2} = 1.01 \times 10^4$ Pa.

5. Conclusions

The pyrolytic behaviour of Tyranno alone and of the Tyranno–alumina compact was investigated under Ar or N_2 atmosphere at 1673–1973 K.

1. Under Ar atmosphere, pyrolysis of Tyranno was suppressed by the presence of alumina powder.
2. Under N_2 atmosphere and at lower temperatures, the pyrolysis of Tyranno alone was suppressed by the formation of a nitrided case. In the presence of alumina powder, the pyrolytic behaviour was similar to that under Ar atmosphere, because the formation of the nitrided case was prevented. At elevated temperature, the pyrolysis was suppressed by the presence of alumina powder.
3. Alumina was reduced by the pyrolytic gas of Tyranno, CO, to evaporate mainly as Al_2O. The evaporation was more vigorous under N_2 atmosphere.
4. The fibre-like AlN deposited on the surface of the Tyranno–alumina compact by reaction between the pyrolytic gas and N_2.
5. When Tyranno pyrolysed in alumina powder, it crystallized into both β-SiC and α-SiC of type 2H.

Acknowledgements

This study was partly supported by a subsidy granted by the Ministry of Education, Science and Culture (No. 07 650 800).

References

1. K. M. PREWO, *Am. Ceram. Soc. Bull.* **68** (1989) 395.
2. L. M. SHEPPARD, *ibid.* **69** (1990) 666.
3. T. SHIMOO, M. SUGIMOTO and K. OKAMURA, *Nippon Kinzokugakkaishi* **54** (1990) 802.
4. *Idem*, *Seramikkusu Ronbunshi* **98** (1990) 1324.
5. T. SHIMOO, M. SUGIMOTO, Y. KAKEHI and K. OKAMURA, *Nippon Kinzokugakkaishi* **55** (1991) 294.
6. T. SHIMOO, Y. KAKEHI, M. SUGIMOTO and K. OKAMURA, *Seramikkusu Ronbunshi* **99** (1991) 401.

7. T. SHIMOO, T. MAEDA and K. OKAMURA, *J. Ceram. Soc. Jpn* **101** (1993) 1274.
8. T. SHIMOO and K. OKAMURA, *ibid.* **104** (1996) 169.
9. T. SHIMOO, J. NISHIDA, Y. KATASE and K. OKAMURA, *J. JSPM* **41** (1994) 799.
10. E. T. TURKDOGAN, "Physical Chemistry of High Temperature Technology" (Academic Press, New York, 1980) pp. 5–26.
11. K. INOMATA and Z. INOUE, *Yogyokyokaishi* **78** (1970) 133.
12. M. MITOMO, K. INOMATA and M. KUMANOMIDO *ibid.* **78** (1970) 224.

Received 10 August 1995
and accepted 18 March 1996